
Language-based Action Concept Spaces Improve Video Self-Supervised Learning

Kanchana Ranasinghe
Stony Brook University
kranasinghe@cs.stonybrook.edu

Michael Ryoo
Stony Brook University
mryoo@cs.stonybrook.edu

Abstract

Recent contrastive language image pre-training has led to learning highly transferable and robust image representations. However, adapting these models to video domains with minimal supervision remains an open problem. We explore a simple step in that direction, using language tied self-supervised learning to adapt an image CLIP model to the video domain. A backbone modified for temporal modeling is trained under self-distillation settings with train objectives operating in an *action concept space*. Feature vectors of various action concepts extracted from a language encoder using relevant textual prompts construct this space. We introduce two train objectives, *concept distillation* and *concept alignment*, that retain generality of original representations while enforcing relations between actions and their attributes. Our approach improves zero-shot and linear probing performance on three action recognition benchmarks.

1 Introduction

Actions in videos are defined by individual objects, their relationships, and interaction. Video self-supervised learning focuses on discovering representations aware of such action attributes directly from video content with no human supervision [1]. Particularly in the case of videos, where manual human annotation can be both expensive and noisy, such self-supervised approaches are invaluable.

A recent variant of self-supervision explores learning with loosely paired image-caption pairs, leading to highly transferable and robust representations such as CLIP [2]. These approaches obtain zero-shot performance often comparable to fully-supervised methods. However, their counterparts in the video domain [3, 4, 5, 6, 7, 8, 9] do not exhibit the same generality. In fact, some approaches training CLIP on videos [9, 10] perform subpar to image-CLIP under zero-shot settings (see Table 2). Such behaviour can be attributed to lesser availability and more noisy nature of labelled (or paired caption) video datasets [1]. This motivates exploration into self-supervised learning (SSL) techniques that can learn from videos under less supervision while utilizing existing image CLIP [2] like representations. Existing state-of-the-art video SSL approaches [11, 12] learn highly transferable representations from videos, but combining these with image CLIP representations is not straightforward. In fact, despite methods like SVT [11] being able to utilize image SSL representations [13] for weight initialization to achieve better performance, using image CLIP representations instead for weight initialization leads to performance subpar to image CLIP (see Table 4). This raises necessity for alternate video SSL approaches compatible with CLIP like image representations and is our key motivation.

In this work, we explore self-supervised learning techniques that can adapt the representations of image CLIP models [2] to the video domain under entirely self-supervised settings dependent on no form of video level labels or captions. Under this setting, natural language can still provide strong cues regarding attributes that compose an action category. Motivated by prior zero-shot action recognition work [14, 15], we leverage this to propose novel language-based self-supervised learning objectives, *concept distillation* and *concept alignment*. Following a standard self-distillation and

multi-view based SSL formulation [13, 11], we introduce language aligned features spaces, *action concept spaces*, where our SSL objectives operate. We also introduce regularization suitable for our language aligned SSL objective to prevent collapse during training. Our resulting framework is termed *Language-based Self-Supervision*, or LSS.

In contrast to existing video self-supervised learning approaches [11, 12], our proposed LSS retains and improves transferability of image CLIP representations better in comparison to existing video SSL approaches [11, 12] (see Tables 1 and 4). As an additional benefit, our language aligned learning framework allows direct zero-shot operation on downstream tasks. Moreover, unlike video CLIP methods with similar zero-shot capabilities [3, 4, 5, 6, 7, 8, 9] that utilize per-video labels / captions for learning, our proposed LSS requires only videos for training.

Our key contributions can be summarized as follows:

- Self-supervised learning paradigm capable of retaining and improving strengths of CLIP like image representations for video domain operation
- Video specific self-supervised learning objectives, namely *concept distillation* and *concept alignment*, that enforce relations between action categories and their visual attributes
- Novel language-based video self-supervised learning framework operating zero-shot on downstream action classification tasks without requiring per-video labels / captions for training

Experiments on HMDB-51 [16], UCF-101 [17], and Kinetics-400 [18] datasets showcase state-of-the-art performance for our learned representations under linear-probing, standard zero-shot, and transductive zero-shot settings.

2 Related Work

Self-Supervised Learning in Videos was initially dominated by pretext tasks specific to the video domain [19, 20, 21, 22, 23, 24, 25, 26, 27, 28, 29, 30]. Recently a shift to contrastive losses led to [31, 32, 33, 34, 35, 36] with some variants focused on video specific view generation [37, 38, 39, 40, 11]. An alternate direction has been masked auto-encoders [12]. To the best of our knowledge, existing video self-supervised learning (SSL) approaches operate purely within the visual domain. By video SSL, we refer to methods that utilize only videos with no paired captions (or labels) for each video during training. In contrast, our proposed LSS learns purely from videos in a self-supervised manner, integrating pre-trained language-image models to learn language aligned representations.

Zero-shot Action Recognition began with manual attribute and feature selection [41, 42, 43, 44, 45] with later works utilizing action word embeddings [14, 15]. The idea of connecting action categories with elaborate descriptions of those actions, within language embedding spaces [46, 47] has been a next step and is closely related to our work. This idea is also explored in image domain to boost zero-shot performance [48]. While our work is inspired by such approaches, in contrast, we use relations between such actions and descriptions as self-supervised signals for learning. Recent image CLIP models [2, 49] are another line of works achieving strong performance on some video classification tasks, with only single frame processing. Multiple approaches build on image CLIP [2] to learn video level representations [9, 50, 51, 52, 10, 53] under fully-supervised settings. While achieving strong performance on the training datasets, their zero-shot improvements over CLIP are minimal or even subpar (see Table 2). Therein, LSS focuses on zero-shot performance under self-supervised settings while retaining (and improving) the generality of the representation space.

Self-training (or semi-supervised learning) methods leverage pseudo-labels on unlabeled data [54, 55, 56] for supervised-fashion training. Recently they have been combined with CLIP models for zero-shot operation [57, 58]. While inspired by such self-training approaches, our proposed LSS differs in its continuous feature space self-distillation, language-based relations enforcing, video domain operation, and cross-dataset transfer for zero-shot operation.

Adapting image-CLIP models to video under fully-supervised settings has gathered much interest [3, 4, 5, 6, 7, 8]. Expanding backbones for temporal modeling, multi-modal fusion, secondary training objectives, partial parameter updates, and scaling-up data are key ideas explored [53, 8]. In contrast, proposed LSS is a first to operate under self-supervised settings using no video level annotations.

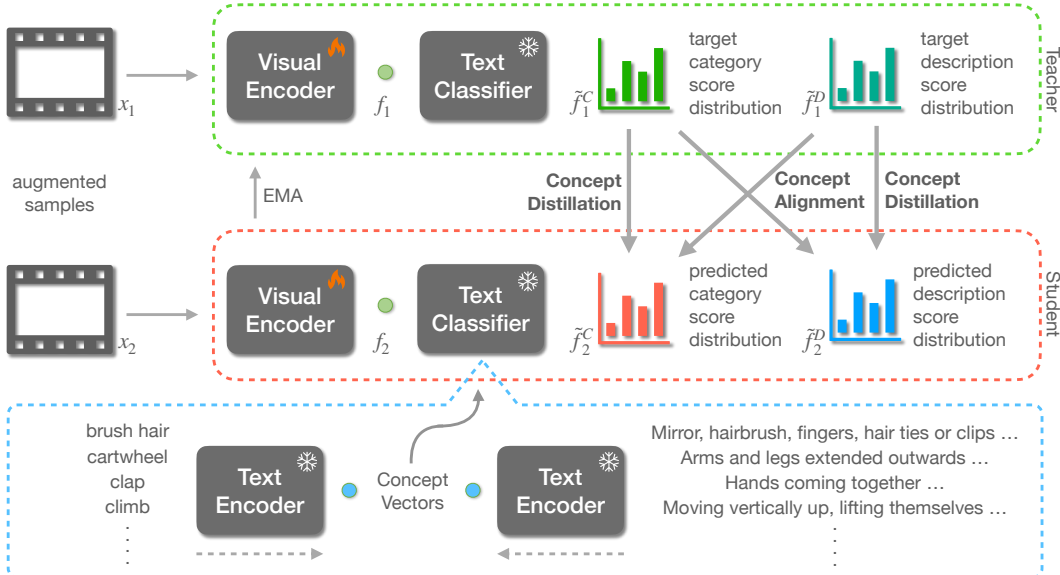


Figure 1: Our overall setup contains three components: visual teacher model (green), visual student model (red), and language model (blue). We utilize the text encoder of CLIP as our language model and extract *concept vectors* relevant to action labels and descriptions of those actions. A visual encoder (containing a space-time backbone) is partially initialized with the visual encoder of CLIP and used to obtain sample specific features. The generated concept vectors are used to project these features to a *concept space* where our proposed *concept distillation* and *concept alignment* losses are applied.

3 Language-based Self-Supervision (LSS)

In this section, we present our proposal, Language-based Self-Supervision (LSS). The generality and robustness of shared image-language representation spaces such as that of CLIP [2] allow interesting manipulations of visual representations using language. We explore such manipulations under the setting of visual self-supervised learning focusing on video understanding. Self-supervised objectives can operate within a latent space constructed with language, retaining language alignment of learned visual representations. This allows better interpretability of representations as well as zero-shot inference. We discuss the four key components of our approach: backbone architecture, concept distillation objective, modifications to avoid collapse, and concept alignment objective.

3.1 Backbone Architecture

Our approach introduces a *text classifier* to self-distillation based SSL works [13, 11], in place of the projector network. Given a data sample x , let $x_1, x_2 \in \mathbb{R}^{(C,T,H,W)}$ be two augmented views generated using video specific transformations following [11], where $C = 3, T = 8, H = W = 224$ are channel, time, and spatial dimensions respectively.

Visual Encoder: A visual encoder, θ_v , processes x_i to produce feature $f_i \in \mathbb{R}^{768}$. We utilize the pre-trained image encoder of CLIP [2] expanded for temporal modelling using factorized space-time attention. The vision transformer variant of CLIP is selected to allow our factorized space-time attention. In particular, we use ViT-B/16 architecture for the the image encoder, in which for a given augmented view with $H = W = 224$ and $T = 8$, each transformer block processes 8 temporal and 196 spatial tokens separately in sequential order, and the embedding dimension of each token is \mathbb{R}^{768} . In addition to the input tokens from the data sample, one classification token [59, 60] serves as the final feature vector output by the network, namely f_i , which is common to the CLIP image encoder. This classification token is inflated and processed suitably following [61] to accommodate our modifications for factorized space-time attention. We follow [61] to zero-initialize additional time-attention parameters, achieving outputs identical to the pre-trained CLIP image encoder at start of training.

Text Classifier: Inspired by [62], a set of n language embeddings extracted from the CLIP text encoder, θ_t , are used to construct the weight parameter of a linear layer (with no bias term), which

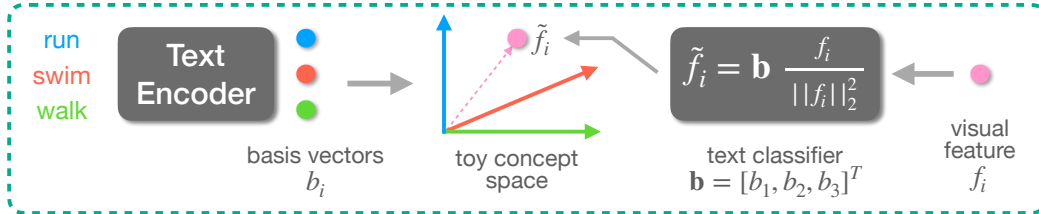


Figure 2: We illustrate a toy concept space constructed with the three action concepts: run, swim, and walk. In this example, the text classifier projects visual feature f_i into the 3-dimensional toy concept space to produce \tilde{f}_i .

we call our text classifier, θ_c . The role of this text classifier is to project visual features f_i to a vector space defined by those n embeddings, producing $\tilde{f}_i \in \mathbb{R}^n$. Next we discuss these vector spaces (referred to as action concept spaces) and the text classifier module in detail.

3.2 Action Concept Spaces

Self-supervised learning approaches following exponential moving average (EMA) based self-distillation [63, 13, 11] utilize a projector network (MLP) to operate in a higher dimensional feature space. This is expected to minimize train-test domain gaps, handle noisy positive sample pairs, and better discriminate nuanced feature differences [64]. Focused on these notions, we propose an alternate *concept space* composed of a set of basis vectors defined by language-based action concepts. Our language-based self-supervision objectives operate within such concept spaces.

Concept Spaces: Building off the assumption that text encoder features capture subtle differences between distinct actions categories, we hypothesize that necessary nuanced distinctions between these actions will be better captured in our proposed concept spaces. The defining parameters of concept spaces are their basis vectors, b_i . Normalized embeddings (extracted from text encoder, θ_t) of various natural language captions (c_i) relevant to action categories are used as these basic vectors.

$$b_i = \theta_t(c_i) / \|\theta_t(c_i)\|_2^2 \quad (1)$$

$$\mathbf{b} = [b_1, b_2, \dots, b_n]^T; \mathbf{b} \in \mathbb{R}^{(n,d)} \quad (2)$$

Note that these basis vectors are not necessarily orthogonal. As illustrated in Fig. 2, a single set of basis vectors, \mathbf{b} , defines one action concept space. We define two sets of basic vectors: action category vectors and action description vectors. Action category vectors relate to a single action label which is converted to a caption using textual prompting following [2]. Action description vectors are averaged embeddings of multiple descriptions and visual characteristics relevant to individual action categories. These two distinct sets of basic vectors lead to two distinct concept spaces which we name *category concept space* and *description concept space* respectively.

Category Concept Space: We construct the category concept space using action labels from Kinetics-400 [18], UCF-101 [17], and HMDB-51 [16] datasets. This leads to a set of 530 (400 + 101 + 51, ignoring overlaps) basis vectors. While expanding the basis vector set with additional action labels is explored and discussed in Section 4, this modest set of 530 was sufficient to gain downstream performance improvements. Further expansion of concept spaces is left as a future direction.

Description Concept Space: This space is constructed conditioned on the previous category concept space. For each action label used in the latter, we extract 4 distinct descriptions and a set of visual characteristics relevant to that action label using a large language model. In detail, we prompt GPT-3 [65] to generate such descriptions and characteristics using procedure outlined in Appendix A. We highlight that GPT-3 is simply used as an intelligent agent to create natural language descriptions given action category labels. The textual outputs generated for each action label are processed by our text encoder to produce multiple embeddings for a single action label. These embeddings are averaged to produce the corresponding basis vector for the description concept space. Note how this leads to a common dimensionality between the two concept spaces as well as one to one correspondences between the basic vectors of the spaces, which we leverage in our self-supervision objectives.

3.3 Concept Distillation

We now describe our primary self-supervised learning objective, concept distillation. Standard multi-view based self-supervision enforces a network to encode the common information between

two augmented (distorted) views of a data sample [64]. This common information can be considered as the augmentation invariant signal present in the original data sample [64, 66]. In the case of self-distillation based approaches [13, 11], a higher dimensional feature space is utilized to enforce the self-supervision objectives. Instead, we propose to use action concept spaces as an alternative.

Proposed concept distillation depends on an action concept space and visual video features aligned to the basis vectors of that space. Given our visual features $f_i \in \mathbb{R}^d$, we obtain projected $\tilde{f}_i \in \mathbb{R}^n$ as,

$$\tilde{f}_i = \mathbf{b} (f_i / \|f_i\|_2) = [b_1 \cdot f'_i, b_2 \cdot f'_i, \dots, b_n \cdot f'_i]^T \quad (3)$$

Similarity Calculation: Projecting normalized visual video features to a concept space corresponds to calculating the dot-product similarity with each basic vector of the concept space. The projected vector \tilde{f}_i can be viewed as a similarity *score distribution* across all basis vectors of the concept space. Inspired by [62], we implement this similarity calculation as a linear layer with weight matrix \mathbf{b} and bias terms zero. We refer to this layer as the *text classifier*. Similar to [62], our text classifier remains frozen (no parameter updates), but in our case, this is to retain the original language distribution.

Concept Distillation Objective: Viewing projected features for two augmented views of a single video as score distributions, we argue that the underlying signal of the original video would relate to a unique score distribution to which score distributions of each view should be similar. Therein, following our EMA teacher based self-distillation setup (see Section 3.1 for details), we enforce the score distribution to be consistent across views. Given two views x_1, x_2 of a single video, our teacher and student visual encoders process them respectively to produce f_1, f_2 . The text classifier projects these to concept space, producing score distributions \hat{f}_1, \hat{f}_2 . We obtain our objective, \mathcal{L}_{CD} as:

$$\hat{f}_i[k] = \frac{\exp(\tilde{f}_i[k]/\lambda_i)}{\sum_{j=1}^n \exp(\tilde{f}_i[j]/\lambda_i)} \quad (4)$$

$$w_s = \max(\hat{f}_1) \quad (5)$$

$$\mathcal{L}_{CD}(\tilde{f}_1, \tilde{f}_2) = -w_s \cdot \sum_{j=1}^n \hat{f}_1[j] \log \hat{f}_2[j] \quad (6)$$

The teacher and student score distributions, \hat{f}_1, \hat{f}_2 , are softmax normalized in Eq. (4), with temperature terms $\lambda_1 = 0.1, \lambda_2 = 1$ for sharpening only the teacher score distribution. A significance score w_s is calculated for each sample in Eq. (5). In the softmax normalized teacher score distribution (\hat{f}_1), the maximum value is high when peaked at a single action concept and low when peaked at multiple action concepts. Considering the noisy nature of multi-peak teacher score distributions, we utilize w_s to minimize their overall effect during training. Our overall \mathcal{L}_{CD} is thus implemented as in Eq. (6).

Distinct Concept Spaces: Given the two distinct action concept spaces defined in Section 3.2, we utilize two parallel text classifiers to implement each, and obtain two score distributions, one for each concept space. Defining score distributions $\tilde{f}_i^C, \tilde{f}_i^D$ for category and description concept spaces respectively, we apply our \mathcal{L}_{CD} on each pair separately to obtain separate losses as follows:

$$\mathcal{L}_{CD}^X = \mathcal{L}_{CD}(\tilde{f}_1^X, \tilde{f}_2^X) \quad (7)$$

We highlight how our concept spaces implemented as text classifiers are maintained intact by freezing the text classifier during training. This allows our approach to perform direct zero-shot inference, making concept distillation additionally advantageous over standard video SSL techniques.

3.4 Uniform Distribution Prior

Avoiding collapse is a key concern in SSL methods [13, 11, 64] and recent self-distillation based approaches utilize feature sharpening and centering operations to avoid collapse [13, 11]. While we similarly perform sharpening operations on the teacher outputs, given the nature of our action concept space, performing a learned vector mean subtraction based centering operations can break the meaningful structure of score distributions. Instead, we enforce a uniform distribution prior on the expected score distribution over the entire training dataset. The centering operation proposed in [13] acts similarly pushing representations towards a uniform distribution while the sharpening operation counters its effect. We approximate expectation over the dataset as a moving average of

mean score distributions at each train iteration and the uniform prior is enforced as:

$$\hat{f}_{\text{MA}}^{\text{X}} = \tau \cdot \hat{f}_2^{\text{X}} + (1 - \tau) \cdot \hat{f}_{\text{MA}} \quad (8)$$

$$\mathcal{L}_{\text{UP}}^{\text{X}} = -\frac{1}{n} \sum_j \log \hat{f}_{\text{MA}}^{\text{X}}[j] \quad (9)$$

where the hyper-parameter $\tau = 0.5$ is fixed during training. We highlight that \mathcal{L}_{UP} is necessary for convergence with concept distillation and is added to the concept distillation objective, $\mathcal{L}_{\text{CD}}^{\text{X}}$.

3.5 Concept Alignment

Aligning action category labels and their descriptions or attributes within some embedding space has been explored in video SSL under multiple settings [46, 47]. Motivated by these promising results, we explore how such alignment can be integrated to improve our framework with *concept spaces*. In Section 3.2, we define two distinct action concept spaces constructed from category labels and detailed category descriptions respectively. We hypothesize that explicit alignment of video features between these two spaces based on their one to one relationship can learn additional information. Therein, we introduce our concept alignment objective, \mathcal{L}_{CA} , as follows:

$$\mathcal{L}_{\text{CA}} = \mathcal{L}_{\text{CD}}(\tilde{f}_1^{\text{C}}, \tilde{f}_2^{\text{D}}) + \mathcal{L}_{\text{CD}}(\tilde{f}_1^{\text{D}}, \tilde{f}_2^{\text{C}}) \quad (10)$$

Overall SSL Objective: Reusing \mathcal{L}_{CD} from Eq. (6), we match score distributions across our two concept spaces instead of within a single concept space. $\mathcal{L}_{\text{CD}}(\tilde{f}_1^{\text{C}}, \tilde{f}_2^{\text{D}})$ aligns student description score distribution \tilde{f}_2^{D} to teacher category score distribution \tilde{f}_1^{C} while $\mathcal{L}_{\text{CD}}(\tilde{f}_1^{\text{D}}, \tilde{f}_2^{\text{C}})$ aligns student category score distribution \tilde{f}_2^{C} to teacher description score distribution \tilde{f}_1^{D} . Combining all terms, we obtain:

$$\mathcal{L} = (\mathcal{L}_{\text{CD}}^{\text{C}} + \mathcal{L}_{\text{UP}}^{\text{C}}) + (\mathcal{L}_{\text{CD}}^{\text{D}} + \mathcal{L}_{\text{UP}}^{\text{D}}) + \mathcal{L}_{\text{CA}} \quad (11)$$

4 Experiments

In this section, we first describe our experimental setup followed by discussion of results for linear probing self-supervised representations and zero-shot analysis.

Datasets: We use three standard action recognition benchmark datasets in our experiments: Kinetics-400 [18], UCF-101 [17], and HMDB-51 [16]. Kinetics-400 is a large-scale dataset containing 240,000 training videos and 20,000 validation videos belonging to 400 different action classes. On average, these videos are of duration around 10 seconds, with 25 frames per second (i.e., around 250 frames per video). UCF-101 and HMDB-51 are small-scale datasets each containing 13k videos (9.5k/3.7k train/test) belonging to 101 classes and 5k (3.5k/1.5k train/test) videos belonging to 51 classes respectively. They also contain similar duration videos.

Self-supervised Training: Our SSL training phase uses the train split of Kinetics-400 dataset [18] *without* using any per-video labels. We train for 15 epochs using a batch size of 32 across 4 NVIDIA-A5000 GPUs using ADAM-W [67, 68] optimizer on the student model with an initial learning rate of $1e - 5$ following a cosine decay schedule. The EMA teacher is updated from student weights after each training iteration with a decay ratio of $2e - 4$. Unless otherwise specified, this model is used for all downstream task evaluations.

Transductive Training: For selected experiments, we additionally perform self-supervised training directly on the train split of each downstream dataset. For Kinetics-400, we follow the same setup described above. In the case of HMDB-51 and UCF-101, we perform self-supervised training for a longer duration of 100 epochs (smaller train sets) leaving all other hyper-parameters unchanged.

View Generation: Our self-supervised setup requires two views of a single video. We sample two clips from a video following global view generation in [11]. In detail, we select two random intervals from a video, and uniformly sample (equal time gaps between frames) 8 frames of 224x224 spatial dimensions from within that interval. Standard video augmentations from [69] are also applied randomly for each view.

Linear Probing: We follow standard linear probing settings on our two downstream datasets to evaluate quality of representations learned by our self-supervised learning phase. We follow the same

Table 1: **Linear Probing on HMDB-51 [16] and UCF-101 [70]:** We compare our method against prior work, reporting top-1 (%) accuracy (following evaluation procedure in [11]). ‘ITP’ stands for image-text pre-training. Gray shaded methods use additional optical flow (OF) inputs for training. Nevertheless, our performance is comparable to such methods using per-video OF modality information. In contrast, we use generic language modality information and require no one-to-one language relations with individual videos during training.

Method	Backbone	ITP	TFLOPS	Frames	Epochs	HMDB	UCF
MemDPC [32] (ECCV '20)	R2D3D-34	✗	-	64	-	30.5	54.1
CoCLR [33] (NeurIPS '20)	S3D	✗	0.07	32	100	52.4	77.8
ELo [30] (CVPR '20)	R(2+1)D	✗	17.5	-	100	-	-
RSPNet [38] (AAAI '21)	S3D-G	✗	0.07	16	200	-	-
VideoMoCo [71] (CVPR '21)	R(2+1)D	✗	17.5	32	200	49.2	78.7
BE [72] (CVPR '21)	I3D	✗	2.22	16	50	-	-
CMD [73] (CVPR '21)	R(2+1)D-26	✗	-	16	120	-	-
CVRL [34] (CVPR '21)	R3D-50	✗	3.19	32	800	57.3	89.2
TCLR [40] (Arxiv '21)	R(2+1)D-18	✗	-	16	100	-	-
MoDist [74] (Arxiv '21)	R3D-50	✗	3.19	8	100	63.0	91.5
BraVe [36] (ICCV '21)	R3D-50	✗	3.19	16	-	68.3	92.5
Vi ² CLR [75] (ICCV '21)	S3D	✗	0.07	32	300	47.3	75.4
ASCNet [37] (ICCV '21)	S3D-G	✗	0.07	64	200	-	-
TEC [76] (ICCV '21)	S3D-G	✗	0.07	32	200	-	-
LSFD [39] (ICCV '21)	C3D	✗	-	16	-	-	-
MCN [77] (ICCV '21)	R3D	✗	3.19	32	50	42.9	73.1
CORP [78] (ICCV '21)	R3D-50	✗	3.19	16	800	58.7	90.2
SVT [11] (CVPR '22)	ViT-B	✗	0.59	16	20	57.8	90.8
VideoMAE [12] (NeurIPS '22)	ViT-B	✗	0.59	16	800	60.3	84.7
MERLOT [79] (NeurIPS '21)	ViT-B	✓	-	16	-	55.4	80.1
VATT [80] (NeurIPS '21)	ViT-B	✓	-	32	-	66.4	87.6
TVTS [81] (CVPR '23)	ViT-B	✓	0.59	16	20	58.4	83.4
LaViLa [82] (CVPR '23)	ViT-L	✓	-	4	5	61.5	88.1
LSS (ours)	ViT-B	✓	0.59	8	20	69.2	91.0

settings in [11] for fair comparison. Our visual encoder is frozen and a randomly initialized linear layer is trained on the train split of the downstream dataset in a fully-supervised manner. We train for 15 epochs using a batch size of 128 across 2 NVIDIA-A5000 GPUs using ADAM-W [67, 68] optimizer with an initial learning rate of $1e - 3$ following a cosine decay schedule. During inference, we sample 3 224x224 dimensional spatial crops with 8 uniformly spaced frames from each video following prior work [11, 34].

Zero-Shot Inference: For zero-shot inference, we project class labels of downstream datasets to our text encoder feature space, and construct an alternate text classifier. Using this text classifier, we make zero-shot predictions. This setup is identical to dot-product similarity based inference in CLIP [2] (explanation in Section 3.3). In line with prior work [11, 34], we feed three 224x224 dimensional spatial crops with 8 uniformly spaced frames sampled from each video to the visual encoder and average its output feature embedding prior to normalized dot-product calculation in the text encoder.

4.1 Linear-Probing Analysis

We first evaluate LSS under linear probing settings on HMDB-51 & UCF-101 datasets. Our results (top-1 accuracy) are reported in Table 1. Our proposed LSS achieves state-of-the-art results on both datasets, outperforming prior approaches. Note that MoDist [74] and BraVe [83], both of which additionally utilize video-level optical flow (OF) for self-supervision, are not directly comparable. Still, our LSS showcases competitive performance to those even without such motion information.

4.2 Zero-Shot Analysis

Our LSS provides the additional advantage of zero-shot operation unlike standard video SSL approaches. To this end, we conduct two forms of zero-shot experiments. First, we evaluate LSS on

Table 2: **Zero-shot Transfer on HMDB-51 [16] and UCF-101 [70]:** We compare LSS against prior work, reporting top-1 accuracy (%). Mean across three test splits is reported following [53]. ‘ITP’ stands for image-text pre-training and ‘Video Labels’ refers to using per-video annotations (or paired captions) for supervision during video-based training. We highlight how among directly comparable unsupervised (at video level) approaches as well as over the CLIP [2] baseline, LSS boosts zero-shot performance.

Method	Backbone	ITP	Video Labels	Frames	HMDB	UCF
TS-GCN [84] _(AAAI '19)	GCN	✗	✓	16	23.2	34.2
E2E [85] _(CVPR '20)	CNN	✗	✓	16	32.7	48.0
ER-ZSAR [46] _(ICCV '21)	CNN	✗	✓	8	35.3	51.8
ActionCLIP [9]	ViT-B	✓	✓	32	40.8	58.3
X-CLIP [10] _(ECCV '22)	ViT-B	✓	✓	32	44.6	72.0
VicTR [53]	ViT-B	✓	✓	32	51.0	72.4
MOV [†] [5]	ViT-B	✓	✓	16	60.8	82.6
MTE [86] _(ECCV '16)	-	✗	✗	-	19.7	15.8
ASR [87] _(ECML '17)	CNN	✗	✗	16	21.8	24.4
ZSECOE [88] _(CVPR '17)	-	✗	✗	-	22.6	15.1
UR [47] _(CVPR '18)	CNN	✗	✗	1	24.4	17.5
CLIP [2] _(ICML '21)	ViT-B	✓	✗	1	46.5	69.8
CLIP [2] _(ICML '21)	ViT-B	✓	✗	8	47.2	70.3
LaViLa [82] _(CVPR '23)	ViT-L	✓	✗	4	16.6	18.2
LSS (ours)	ViT-B	✓	✗	8	49.5	72.0

Table 3: **Transductive Zero-shot Transfer on HMDB-51 [16], UCF-101 [70], and Kinetics-400 [18]:** We report top-1 accuracy (%) following the evaluation procedure in [53]. Similar to prior work, we perform dataset specific unsupervised fine-tuning (using our self-supervised objective) on the train-splits of each downstream dataset (no labels used). ‘ITP’ refers to image-text pretraining, and ‘Video Labels’ refers to video level supervised training. Note that CLIP [2] is not transductive and is included only for comparison purposes.

Method	Backbone	ITP	Video Labels	Frames	HMDB	UCF	K400
UR [47] _(CVPR '18)	CNN	✗	✗	1	28.9	20.1	-
TS-GCN [84] _(AAAI '19)	GCN	✗	✓	16	23.2	34.2	-
CLIP [2] _(ICML '21)	ViT-B	✓	✗	8	47.2	70.3	49.7
MUST [57] _(ICLR '23)	ViT-B	✓	✗	1	48.9	81.1	51.2
LSS (ours)	ViT-B	✓	✗	8	55.0	75.6	54.3

standard zero-shot classification, where our model trained on Kinetics-400 (under SSL settings) is evaluated on the two downstream datasets, HMDB-51 and UCF-101. We report these results (top-1 accuracy) in Table 2. Compared to prior work utilizing per-video labels / captions for training, we achieve competitive performance. We note that MOV [5] trained under supervised settings with per-video labels and additional audio information is not a direct comparison.

In contrast to most prior approaches, LSS uses no video level labels for its Kinetics-400 training. In particular, LSS has not seen any labelled videos during its training process. Compared to prior work operating under these settings, LSS achieves state-of-the-art performance on both downstream datasets as seen in the bottom half of Table 2.

An alternate setting in prior zero-shot work is transductive training, where self-supervised learning is performed directly on train splits of downstream datasets. Under this setting, we evaluate on all three datasets, Kinetics-400, HMDB-51, and UCF-101, reporting results (top-1 accuracy) in Table 3. In the case of HMDB-51 and Kinetics-400, our method achieves state-of-the-art performance. For UCF-101, we achieve competitive results, and clear improvements over a CLIP [2] baseline.

4.3 Ablations

We next study the contribution of each components within our approach. All ablative experiments follow the same SSL phase on the Kinetics-400 train set (as described in Section 4) followed by

Table 4: **Ablation on SSL objectives:** We ablate our proposed concept distillation (CD) applied on category (CD^C) and description (CD^D) concept spaces and concept alignment (CA) using linear probing (LP) & zero-shot transfer (ZS) on HMDB-51 [16] dataset. Since our approach cannot be trained without any objective, we construct two new baselines from CLIP [2] and SVT [11] (details in Section 4.3). Each proposed component obtains clear improvements over the baselines.

	CD^C	CD^D	CA	LP	ZS
CLIP	✗	✗	✗	63.9	46.5
CLIP [†]	✗	✗	✗	67.3	47.2
SVT [§]	✗	✗	✗	62.2	-
Ours	✓	✗	✗	68.5	48.8
Ours	✓	✓	✗	69.0	49.2
Ours	✓	✓	✓	69.2	49.5

Table 5: **Ablation on concept space construction:** We explore two extensions to our concept spaces and evaluate using zero-shot transfer on validation splits of HMDB-51 [16] and UCF-101 [17] datasets. We vary the set of n action categories or descriptions used for constructing each concept space (see Section 4.3 for details). For 2000 words, we utilize 1000 most common nouns and verbs from WordNet [89, 90] and for 10,000 sentences we similarly select example sentences for action verbs from WordNet [89, 90]. Our selected approach is highlighted in Gray. The results appear inconclusive leaving further exploration for future.

Concept Space	HMDB	UCF
K400+UCF+HMDB	49.5	72.0
+ 2000 words	48.6	71.8
+ 10,000 sentences	49.6	71.4

zero-shot analysis on validation sets of HMDB-51 and UCF-101. In the case of linear probing results, training is conducted following same settings (see Section 4) on the train set of HMDB-51 followed by evaluation on its validation set.

SSL Objectives: First we ablate each proposed component in Eq. (11) and report results in Table 4. In addition to a direct CLIP [2] baseline, we construct two additional baselines building off CLIP [2] and SVT [11] for better comparison. CLIP[†] baseline applies our backbone modifications (for temporal modeling) with no training, which is identical to averaging per-frame visual encoder features. SVT[§] baseline performs SVT [11] training with CLIP visual encoder initialization (note that language alignment breaks and zero-shot operation is not possible for this baseline). In comparison to the CLIP baselines, each proposed component, concept distillation in category and description concept spaces as well as concept alignment, leads to improvements. The comparison against SVT[§] highlights how our SSL approach better preserves language aligned information (contained in CLIP) that is useful even in linear probing. In contrast, the lower performance of SVT[§] compared to CLIP baselines indicates that generic SSL techniques may be losing useful information contained in CLIP.

Concept Spaces: Our next focus is on construction of concept spaces. We explore how separately augmenting each concept space affects downstream task performance measured with zero-shot transfer. These results are reported in Table 5. First, focused on the category concept space, we construct additional category labels using 1000 most common nouns and verbs each (total of 2000) from the WordNet dataset [89, 90]. Next, we augment the description concept space using 10,000 sentences. We select these from example sentences provided for action verbs in the WordNet dataset [89, 90]. In these experiments, only the concept distillation objective is applied on these augmented spaces and concept alignment operates only on the base category set. This is because independently augmenting one of the action spaces eliminates their shared and aligned dimensionality. Results for these two settings are reported in row 2 & 3 respectively in Table 5.

5 Conclusion

We introduce a novel language-based self-supervised learning (SSL) approach for videos, termed LSS, capable of adapting strong language-aligned image representations (CLIP [2]) to the video domain. In particular, we propose two self-distillation based SSL objectives, *concept distillation* and *concept alignment*. Our approach trains with no video level labels or paired captions similar to prior video SSL works, but retains language alignment from image CLIP enabling direct zero-shot inference. We demonstrate state-of-the-art performance in terms of linear probing with the learned representations on downstream tasks. For zero-shot operation, LSS demonstrates strong performance under both standard and transductive settings, indicating a promising direction for video SSL.

Limitations & Broader Impact: Language alignment of LSS is limited to per-frame static information since the alignment is derived from image CLIP. LSS cannot distinguish motion based categories like "moving object left to right". We leave this for future work. In terms of broader impact, datasets and pre-trained models used possibly contain biases, which may be reflected in LSS. However, our reduced reliance on human annotations may lower additional biases.

Reproducibility Statement: We build a codebase derived from source code of SVT [11] & CLIP [2] and use pre-trained CLIP weights from <https://github.com/openai>. All experiments use publicly available datasets. Our action descriptions will be released publicly along with our codebase.

APPENDIX

A Prompting details

Our proposed approach utilizes two sets of language based captions: categories and descriptions. While categories are obtained directly from the class labels of datasets (set of unique labels - e.g. 400 classes in Kinetics-400 dataset), the descriptions are generated automatically utilizing GPT-3 [65]. For each category caption, we query GPT-3 to provide a set of descriptions and visual characteristics. In detail, we use the following two prompts to generate descriptions and visual characteristics:
 prompt1 = "Give 4 different descriptions for the phrase: {category}?"
 prompt2 = "List visual objects or characteristics usually seen with the action: {category}?"
 The resulting two sets of captions are converted to text embeddings using our text-encoder, and a single average text embedding is computed. This averaged embedding is used as the description basis vector for that category. Also, the resulting dataset containing these category-description pairs is made available publicly.

B Additional Experiments

Smaller Concept Set: We explore how using a smaller set of basis vectors to construct our concept spaces affects final performance. These results are present in Table 6. Our results indicate that using only Kinetics-400 dataset category labels (without including those from UCF-101 and HMDB-51) leads to minimal decrease in performance and an improvement over the baseline.

Linear Probing Evaluation: We present more results for linear probing in Table 7. Our proposed LSS improves over the baseline and achieves competitive performance on the Kinetics-400 dataset.

Table 6: **Further Ablation on concept spaces:** We explore how using only the Kinetics-400 (K400) base classes in our concept space affects zero-shot accuracy on HMDB-51 and UCF-101 datasets. A CLIP baseline (modified for video domain without re-training) is reported in row 1 for comparison purposes. Results in row 2 indicate how our method boosts accuracy over the baseline when using only K400 classes as concept vectors. However, including more labels as concept vectors (our default setting) further improves performance as seen in row 3.

Concept Space	HMDB	UCF
CLIP	47.2	70.3
K400	48.4	71.1
K400+UCF+HMDB	49.5	72.0

Table 7: We report top-1 (%) accuracy on the Kinetics-400 [18] validation set for linear probing evaluation. All models are pre-trained on the training set of Kinetics-400 dataset. We also report a CLIP baseline for comparison purposes. Performance of our proposed approach is on-par with prior state-of-the-art and showcases improvements over our baseline method.

Method	Backbone	Linear
CVRL [34] (CVPR'21)	R3D-101	67.6
BraVe [36] (ICCV'21)	R3D-50	66.7
Vi ² CLR [75] (ICCV'21)	S3D	63.4
CORP [78] (ICCV'21)	R3D-50	66.6
SVT [11] (CVPR'22)	ViT-B	68.1
VideoMAE [12] (NeurIPS'22)	ViT-B	61.3
CLIP [2]	ViT-B	66.4
LSS (ours)	ViT-B	67.3

C Significance Weight in Concept Distillation

In Eq. (6), we utilize a significance weight term, W_s , which represents the confidence of the target concept space projection for a given sample. We note how each sample during training is a clip sampled from a video (which covers a temporal crop of video). Our intuition for this weight is to act as a way of prioritizing more important clips over the less important ones.

D Limitations & Future Work

The language alignment of our learned representations are derived from image CLIP [2]. While containing highly discriminative and generic information at image level, such CLIP features lack spatial awareness at an object level [91]. Our proposed model building off these representations is inherently limited in understanding object level motion and interaction within videos. However, recent progress in localization aware CLIP models [91, 92, 93] opens avenues for leveraging their object-centric or pixel-level representations to better model such video motion patterns. We hope to explore this as a key future direction.

References

- [1] Madeline Chantry Schiappa, Yogesh Singh Rawat, and Mubarak Shah. Self-supervised learning for videos: A survey. *ACM Computing Surveys*, 2022. 1
- [2] Alec Radford, Jong Wook Kim, Chris Hallacy, Aditya Ramesh, Gabriel Goh, Sandhini Agarwal, Girish Sastry, Amanda Askell, Pamela Mishkin, Jack Clark, et al. Learning Transferable Visual Models From Natural Language Supervision. In *ICML*, pages 8748–8763. PMLR, 2021. 1, 2, 3, 4, 7, 8, 9, 10, 11
- [3] Hongwei Xue, Yuchong Sun, Bei Liu, Jianlong Fu, Ruihua Song, Houqiang Li, and Jiebo Luo. CLIP-ViP: Adapting Pre-trained Image-Text Model to Video-Language Representation Alignment. *arXiv preprint arXiv:2209.06430*, 2022. 1, 2
- [4] Shen Yan, Tao Zhu, Zirui Wang, Yuan Cao, Mi Zhang, Soham Ghosh, Yonghui Wu, and Jiahui Yu. Video-Text Modeling with Zero-Shot Transfer from Contrastive Captioners. *arXiv preprint arXiv:2212.04979*, 2022. 1, 2
- [5] Rui Qian, Yeqing Li, Zheng Xu, Ming-Hsuan Yang, Serge Belongie, and Yin Cui. Multimodal Open-Vocabulary Video Classification via Pre-Trained Vision and Language Models. *arXiv preprint arXiv:2207.07646*, 2022. 1, 2, 8
- [6] Chen Ju, Tengda Han, Kunhao Zheng, Ya Zhang, and Weidi Xie. Prompting Visual-Language Models for Efficient Video Understanding. In *ECCV*, pages 105–124. Springer, 2022. 1, 2
- [7] Hanoona Rasheed, Muhammad Uzair Khattak, Muhammad Maaz, Salman Khan, and Fahad Shahbaz Khan. Fine-tuned CLIP Models are Efficient Video Learners. *arXiv preprint arXiv:2212.03640*, 2022. 1, 2
- [8] Feng Cheng, Xizi Wang, Jie Lei, David Crandall, Mohit Bansal, and Gedas Bertasius. VindLU: A Recipe for Effective Video-and-Language Pretraining. *arXiv preprint arXiv:2212.05051*, 2022. 1, 2
- [9] Mengmeng Wang, Jiazheng Xing, and Yong Liu. ActionCLIP: A New Paradigm for Video Action Recognition. *arXiv preprint arXiv:2109.08472*, 2021. 1, 2, 8
- [10] Bolin Ni, Houwen Peng, Minghao Chen, Songyang Zhang, Gaofeng Meng, Jianlong Fu, Shiming Xiang, and Haibin Ling. Expanding language-image pretrained models for general video recognition. In *European Conference on Computer Vision*, 2022. 1, 2, 8
- [11] Kanchana Ranasinghe, Muzammal Naseer, Salman Hameed Khan, Fahad Shahbaz Khan, and Michael S. Ryoo. Self-supervised video transformer. *2022 IEEE/CVF Conference on Computer Vision and Pattern Recognition (CVPR)*, pages 2864–2874, 2021. 1, 2, 3, 4, 5, 6, 7, 9, 10
- [12] Zhan Tong, Yibing Song, Jue Wang, and Limin Wang. Videomae: Masked autoencoders are data-efficient learners for self-supervised video pre-training. *ArXiv*, abs/2203.12602, 2022. 1, 2, 7, 10
- [13] Mathilde Caron, Hugo Touvron, Ishan Misra, Hervé Jégou, Julien Mairal, Piotr Bojanowski, and Armand Joulin. Emerging properties in self-supervised vision transformers. In *ICCV*, 2021. 1, 2, 3, 4, 5
- [14] Biagio Brattoli, Joseph Tighe, Fedor Zhdanov, Pietro Perona, and Krzysztof Chalupka. Rethinking zero-shot video classification: End-to-end training for realistic applications. In *CVPR*, 2020. 1, 2
- [15] Xun Xu, Timothy Hospedales, and Shaogang Gong. Transductive zero-shot action recognition by word-vector embedding. *IJCV*, 2017. 1, 2

- [16] Hildegard Kuehne, Hueihan Jhuang, Estíbaliz Garrote, Tomaso Poggio, and Thomas Serre. HMDB: A large video database for human motion recognition. In *ICCV*, pages 2556–2563. IEEE, 2011. 2, 4, 6, 7, 8, 9
- [17] Khurram Soomro, Amir Roshan Zamir, and Mubarak Shah. UCF101: A dataset of 101 human actions classes from videos in the wild. *Arxiv*, 2012. 2, 4, 6, 9
- [18] Joao Carreira and Andrew Zisserman. Quo vadis, action recognition? A new model and the Kinetics dataset. In *CVPR*, 2017. 2, 4, 6, 8, 10
- [19] Michael Mathieu, Camille Couprie, and Yann LeCun. Deep multi-scale video prediction beyond mean square error. In *ICLR*, 2016. 2
- [20] Viorica Pătrăucean, Ankur Handa, and Roberto Cipolla. Spatio-temporal video autoencoder with differentiable memory. In *ICLR (Workshop)*, 2016. 2
- [21] Jacob Walker, Carl Doersch, Abhinav Gupta, and Martial Hebert. An uncertain future: Forecasting from static images using variational autoencoders. In *ECCV*, 2016. 2
- [22] Nitish Srivastava, Elman Mansimov, and Ruslan Salakhudinov. Unsupervised learning of video representations using lstms. In *ICML*, 2015. 2
- [23] Carl Vondrick, Hamed Pirsiavash, and Antonio Torralba. Generating videos with scene dynamics. In *NeurIPS*, 2016. 2
- [24] Carl Vondrick, Abhinav Shrivastava, Alireza Fathi, Sergio Guadarrama, and Kevin Murphy. Tracking emerges by coloring videos. In *ECCV*, 2018. 2
- [25] Pulkit Agrawal, Joao Carreira, and Jitendra Malik. Learning to see by moving. In *ICCV*, 2015. 2
- [26] Ross Goroshin, Joan Bruna, Jonathan Tompson, David Eigen, and Yann LeCun. Unsupervised learning of spatiotemporally coherent metrics. In *ICCV*, 2015. 2
- [27] Phillip Isola, Daniel Zoran, Dilip Krishnan, and Edward H. Adelson. Learning visual groups from co-occurrences in space and time. In *ICLR*, 2016. 2
- [28] Ishan Misra, C. Lawrence Zitnick, and Martial Hebert. Shuffle and learn: Unsupervised learning using temporal order verification. In *ECCV*, 2016. 2
- [29] Xiaolong Wang and Abhinav Gupta. Unsupervised learning of visual representations using videos. In *ICCV*, 2015. 2
- [30] AJ Piergiovanni, Anelia Angelova, and Michael S. Ryoo. Evolving losses for unsupervised video representation learning. In *CVPR*, 2020. 2, 7
- [31] Christoph Feichtenhofer, Haoqi Fan, Bo Xiong, Ross Girshick, and Kaiming He. A large-scale study on unsupervised spatiotemporal representation learning. *Arxiv*, 2021. 2
- [32] Tengda Han, Weidi Xie, and Andrew Zisserman. Video representation learning by dense predictive coding. In *ICCV*, 2019. 2, 7
- [33] Tengda Han, Weidi Xie, and Andrew Zisserman. Self-supervised Co-training for Video Representation Learning. *NeurIPS*, 33:5679–5690, 2020. 2, 7
- [34] Rui Qian, Tianjian Meng, Boqing Gong, Ming-Hsuan Yang, Huisheng Wang, Serge Belongie, and Yin Cui. Spatiotemporal contrastive video representation learning. *CVPR*, 2021. 2, 7, 10
- [35] R Devon et al. Representation learning with video deep infomax. *Arxiv*, 2020. 2
- [36] Adrià Recasens, Pauline Luc, Jean-Baptiste Alayrac, Luyu Wang, Florian Strub, Corentin Tallec, Mateusz Malinowski, Viorica Patraucean, Florent Alché, Michal Valko, et al. Broaden your views for self-supervised video learning. *ICCV*, 2021. 2, 7, 10
- [37] Deng Huang, Wenhao Wu, Weiwen Hu, Xu Liu, Dongliang He, Zhihua Wu, Xiangmiao Wu, Mingkui Tan, and Errui Ding. Ascnet: Self-supervised video representation learning with appearance-speed consistency. In *ICCV*, 2021. 2, 7
- [38] Peihao Chen, Deng Huang, Dongliang He, Xiang Long, Runhao Zeng, Shilei Wen, Mingkui Tan, and Chuang Gan. Rspnet: Relative speed perception for unsupervised video representation learning. In *AAAI*, volume 1, 2021. 2, 7
- [39] Nadine Behrmann, Mohsen Fayyaz, Juergen Gall, and Mehdi Noroozi. Long short view feature decomposition via contrastive video representation learning. In *ICCV*, 2021. 2, 7
- [40] Ishan Rajendra Dave, Rohit Gupta, Mamshad Nayeem Rizve, and Mubarak Shah. TCLR: Temporal contrastive learning for video representation. *Arxiv*, 2021. 2, 7
- [41] Jingen Liu, Benjamin Kuipers, and Silvio Savarese. Recognizing human actions by attributes. In *CVPR*, 2011. 2

- [42] Rowan Zellers and Yejin Choi. Zero-shot activity recognition with verb attribute induction. *arXiv preprint arXiv:1707.09468*, 2017. 2
- [43] Mihir Jain, Jan C Van Gemert, Thomas Mensink, and Cees GM Snoek. Objects2action: Classifying and localizing actions without any video example. In *ICCV*, 2015. 2
- [44] Junyu Gao, Tianzhu Zhang, and Changsheng Xu. I know the relationships: Zero-shot action recognition via two-stream graph convolutional networks and knowledge graphs. In *AAAI*, 2019. 2
- [45] Junyu Gao, Tianzhu Zhang, and Changsheng Xu. Learning to model relationships for zero-shot video classification. *TPAMI*, 2020. 2
- [46] Shizhe Chen and Dong Huang. Elaborative Rehearsal for Zero-shot Action Recognition. In *ICCV*, pages 13638–13647, 2021. 2, 6, 8
- [47] Yi Zhu, Yang Long, Yu Guan, Shawn Newsam, and Ling Shao. Towards Universal Representation for Unseen Action Recognition. In *CVPR*, pages 9436–9445, 2018. 2, 6, 8
- [48] Sachit Menon and Carl Vondrick. Visual Classification via Description from Large Language Models. *arXiv preprint arXiv:2210.07183*, 2022. 2
- [49] Chao Jia, Yinfei Yang, Ye Xia, Yi-Ting Chen, Zarana Parekh, Hieu Pham, Quoc Le, Yun-Hsuan Sung, Zhen Li, and Tom Duerig. Scaling Up Visual and Vision-Language Representation Learning With Noisy Text Supervision. In *ICML*, pages 4904–4916. PMLR, 2021. 2
- [50] Huaishao Luo, Lei Ji, Ming Zhong, Yang Chen, Wen Lei, Nan Duan, and Tianrui Li. CLIP4Clip: An Empirical Study of CLIP for End to End Video Clip Retrieval. *Neurocomputing*, 508:293–304, 2022. 2
- [51] Max Bain, Arsha Nagrani, Gül Varol, and Andrew Zisserman. A CLIP-Hitchhiker’s Guide to Long Video Retrieval. *arXiv preprint arXiv:2205.08508*, 2022. 2
- [52] Ziyi Lin, Shijie Geng, Renrui Zhang, Peng Gao, Gerard de Melo, Xiaogang Wang, Jifeng Dai, Yu Qiao, and Hongsheng Li. Frozen CLIP Models are Efficient Video Learners. *arXiv preprint arXiv:2208.03550*, 2022. 2
- [53] Kumara Kahatapitiya, Anurag Arnab, Arsha Nagrani, and Michael S. Ryoo. Victr: Video-conditioned text representations for activity recognition. *ArXiv*, abs/2304.02560, 2023. 2, 8
- [54] Antti Tarvainen and Harri Valpola. Mean teachers are better role models: Weight-averaged consistency targets improve semi-supervised deep learning results. In *NIPS*, pages 1195–1204, 2017. 2
- [55] Kihyuk Sohn, David Berthelot, Chun-Liang Li, Zizhao Zhang, Nicholas Carlini, Ekin D Cubuk, Alex Kurakin, Han Zhang, and Colin Raffel. Fixmatch: Simplifying semi-supervised learning with consistency and confidence. In *NeurIPS*, 2020. 2
- [56] David Berthelot, Nicholas Carlini, Ekin D. Cubuk, Alex Kurakin, Kihyuk Sohn, Han Zhang, and Colin Raffel. Remixmatch: Semi-supervised learning with distribution alignment and augmentation anchoring. In *ICLR*, 2020. 2
- [57] Junnan Li, Silvio Savarese, and Steven C. H. Hoi. Masked unsupervised self-training for zero-shot image classification. *ArXiv*, abs/2206.02967, 2022. 2, 8
- [58] Jonathan Kahana, Niv Cohen, and Yedid Hoshen. Improving zero-shot models with label distribution priors. *ArXiv*, abs/2212.00784, 2022. 2
- [59] Jacob Devlin, Ming-Wei Chang, Kenton Lee, and Kristina Toutanova. Bert: Pre-training of deep bidirectional transformers for language understanding. *Arxiv*, 2018. 3
- [60] Alexey Dosovitskiy, Lucas Beyer, Alexander Kolesnikov, Dirk Weissenborn, Xiaohua Zhai, Thomas Unterthiner, Mostafa Dehghani, Matthias Minderer, Georg Heigold, Sylvain Gelly, et al. An image is worth 16x16 words: Transformers for image recognition at scale. *ICLR*, 2021. 3
- [61] Gedas Bertasius, Heng Wang, and Lorenzo Torresani. Is Space-Time Attention All You Need for Video Understanding? In *ICML*, page 4, 2021. 3
- [62] Wenhao Wu, Zhun Sun, and Wanli Ouyang. Revisiting Classifier: Transferring Vision-Language Models for Video Recognition. *AAAI*, 2023. 3, 5
- [63] Jean-Bastien Grill, Florian Strub, Florent Altché, Corentin Tallec, Pierre H Richemond, Elena Buchatskaya, Carl Doersch, Bernardo Avila Pires, Zhaohan Daniel Guo, Mohammad Gheshlaghi Azar, et al. Bootstrap your own latent: A new approach to self-supervised learning. In *NeurIPS*, 2020. 4
- [64] Randall Balestriero, Mark Ibrahim, Vlad Sobal, Ari S. Morcos, Shashank Shekhar, Tom Goldstein, Florian Bordes, Adrien Bardes, Grégoire Mialon, Yuandong Tian, Avi Schwarzschild, Andrew Gordon Wilson, Jonas Geiping, Quentin Garrido, Pierre Fernandez, Amir Bar, Hamed Pirsiavash, Yann LeCun, and Micah Goldblum. A cookbook of self-supervised learning. *ArXiv*, abs/2304.12210, 2023. 4, 5

- [65] Tom B. Brown, Benjamin Mann, Nick Ryder, Melanie Subbiah, Jared Kaplan, Prafulla Dhariwal, Arvind Neelakantan, Pranav Shyam, Girish Sastry, Amanda Askell, Sandhini Agarwal, Ariel Herbert-Voss, Gretchen Krueger, Tom Henighan, Rewon Child, Aditya Ramesh, Daniel M. Ziegler, Jeffrey Wu, Clemens Winter, Christopher Hesse, Mark Chen, Eric Sigler, Mateusz Litwin, Scott Gray, Benjamin Chess, Jack Clark, Christopher Berner, Sam McCandlish, Alec Radford, Ilya Sutskever, and Dario Amodei. Language models are few-shot learners, 2020. [4](#), [10](#)
- [66] Adrien Bardes, Jean Ponce, and Yann LeCun. Vicreg: Variance-invariance-covariance regularization for self-supervised learning. *ArXiv*, abs/2105.04906, 2021. [5](#)
- [67] Diederik P. Kingma and Jimmy Ba. Adam: A method for stochastic optimization. In *ICLR*, 2015. [6](#), [7](#)
- [68] Ilya Loshchilov and Frank Hutter. Decoupled Weight Decay Regularization. *ICLR*, 2019. [6](#), [7](#)
- [69] Rui Qian, Tianjian Meng, Boqing Gong, Ming-Hsuan Yang, Huisheng Wang, Serge Belongie, and Yin Cui. Spatiotemporal Contrastive Video Representation Learning. In *CVPR*, pages 6964–6974, 2021. [6](#)
- [70] Khurram Soomro, Amir Roshan Zamir, and Mubarak Shah. UCF101: A Dataset of 101 Human Actions Classes From Videos in The Wild. *arXiv preprint arXiv:1212.0402*, 2012. [7](#), [8](#)
- [71] Tian Pan, Yibing Song, Tianyu Yang, Wenhao Jiang, and Wei Liu. Videomoco: Contrastive video representation learning with temporally adversarial examples. In *CVPR*, 2021. [7](#)
- [72] Jinpeng Wang, Yuting Gao, Ke Li, Yiqi Lin, Andy J Ma, Hao Cheng, Pai Peng, Rongrong Ji, and Xing Sun. Removing the background by adding the background: Towards background robust self-supervised video representation learning. In *CVPR*, 2021. [7](#)
- [73] Lianghua Huang, Yu Liu, Bin Wang, Pan Pan, Yinghui Xu, and Rong Jin. Self-supervised video representation learning by context and motion decoupling. *CVPR*, 2021. [7](#)
- [74] Fanyi Xiao, Joseph Tighe, and Davide Modolo. Modist: Motion distillation for self-supervised video representation learning. *Arxiv*, 2021. [7](#)
- [75] Ali Diba, Vivek Sharma, Reza Safdari, Dariush Lotfi, Saquib Sarfraz, Rainer Stiefelhagen, and Luc Van Gool. Vi2clr: Video and image for visual contrastive learning of representation. In *ICCV*, 2021. [7](#), [10](#)
- [76] Simon Jenni and Hailin Jin. Time-equivariant contrastive video representation learning. In *ICCV*, 2021. [7](#)
- [77] Yuanze Lin, Xun Guo, and Yan Lu. Self-supervised video representation learning with meta-contrastive network. In *ICCV*, 2021. [7](#)
- [78] Kai Hu, Jie Shao, Yuan Liu, Bhiksha Raj, Marios Savvides, and Zhiqiang Shen. Contrast and order representations for video self-supervised learning. In *ICCV*, 2021. [7](#), [10](#)
- [79] Rowan Zellers, Ximing Lu, Jack Hessel, Youngjae Yu, Jae Sung Park, Jize Cao, Ali Farhadi, and Yejin Choi. Merlot: Multimodal neural script knowledge models. *ArXiv*, abs/2106.02636, 2021. [7](#)
- [80] Hassan Akbari, Linagzhe Yuan, Rui Qian, Wei-Hong Chuang, Shih-Fu Chang, Yin Cui, and Boqing Gong. Vatt: Transformers for multimodal self-supervised learning from raw video, audio and text. *ArXiv*, abs/2104.11178, 2021. [7](#)
- [81] Ziyun Zeng, Yuying Ge, Xihui Liu, Bin Chen, Ping Luo, Shutao Xia, and Yixiao Ge. Learning transferable spatiotemporal representations from natural script knowledge. *ArXiv*, abs/2209.15280, 2022. [7](#)
- [82] Yue Zhao, Ishan Misra, Philipp Krahenbuhl, and Rohit Girdhar. Learning video representations from large language models. *ArXiv*, abs/2212.04501, 2022. [7](#), [8](#)
- [83] Adria Recasens, Pauline Luc, Jean-Baptiste Alayrac, Luyu Wang, Florian Strub, Corentin Tallec, Mateusz Malinowski, Viorica Pătrăucean, Florent Altché, Michal Valko, et al. Broaden Your Views for Self-Supervised Video Learning. In *ICCV*, pages 1255–1265, 2021. [7](#)
- [84] Junyu Gao, Tianzhu Zhang, and Changsheng Xu. I Know the Relationships: Zero-Shot Action Recognition via Two-Stream Graph Convolutional Networks and Knowledge Graphs. In *AAAI*, pages 8303–8311, 2019. [8](#)
- [85] Biagio Brattoli, Joseph Tighe, Fedor Zhdanov, Pietro Perona, and Krzysztof Chalupka. Rethinking Zero-shot Video Classification: End-to-end Training for Realistic Applications. In *CVPR*, pages 4613–4623, 2020. [8](#)
- [86] Xun Xu, Timothy M Hospedales, and Shaogang Gong. Multi-Task Zero-Shot Action Recognition with Prioritised Data Augmentation. In *ECCV*, pages 343–359. Springer, 2016. [8](#)
- [87] Qian Wang and Ke Chen. Alternative Semantic Representations for Zero-Shot Human Action Recognition. In *ECML-PKDD*, pages 87–102. Springer, 2017. [8](#)
- [88] Jie Qin, Li Liu, Ling Shao, Fumin Shen, Bingbing Ni, Jiaxin Chen, and Yunhong Wang. Zero-Shot Action Recognition with Error-Correcting Output Codes. In *CVPR*, pages 2833–2842, 2017. [8](#)
- [89] George A Miller. Wordnet: a lexical database for english. In *Communications of the ACM*, pages 39–41. ACM, 1995. [9](#)

- [90] Christiane Fellbaum. Wordnet and wordnets. In Keith Brown et al., editors, *Encyclopedia of Language & Linguistics*, pages 665–670. Elsevier, 2nd edition, 2005. 9
- [91] Kanchana Ranasinghe, Brandon McKinzie, Sachin Ravi, Yinfei Yang, Alexander Toshev, and Jonathon Shlens. Perceptual grouping in contrastive vision-language models. *ICCV*, 2023. 11
- [92] Jilan Xu, Junlin Hou, Yuejie Zhang, Rui Feng, Yi Wang, Yu Qiao, and Weidi Xie. Learning open-vocabulary semantic segmentation models from natural language supervision. *ArXiv*, 2023. 11
- [93] Jiarui Xu, Shalini De Mello, Sifei Liu, Wonmin Byeon, Thomas Breuel, Jan Kautz, and Xiaolong Wang. GroupViT: Semantic Segmentation Emerges from Text Supervision. In *CVPR*, pages 18134–18144, 2022. 11